Journal of Thermal Analysis and Calorimetry (2021) 143:1037–1050
https://doi.org/10.1007/s10973-020-10041-1

Experimental measurement of viscosity and electrical conductivity of water-based γ-Al_2O_3/MWCNT hybrid nanofluids with various particle mass ratios

S. O. Giwa[1,2] · Mohsen Sharifpur[1,3] · Josua P. Meyer[1] · Somchai Wongwises[4,5] · Omid Mahian[6,7]

Received: 29 March 2020 / Accepted: 3 July 2020 / Published online: 21 July 2020

Abstract

The hybridization of nanoparticles is a concept employed for the improvement of the thermal properties of nanofluids. Presently, there is a scarcity of studies in the open literature concerning the influence of particle mass ratios of hybrid nanofluids on the thermal properties. Thus, this paper investigated the effect of temperatures (15–55 °C) and particle mass ratios (90:10, 80:20, 60:40, 40:60, and 20:80) on the viscosity and electrical conductivity of deionized water (DIW)-based γ-Al_2O_3 and MWCNT hybrid nanofluids. A two-process strategy was deployed to prepare the hybrid nanofluids at a volume concentration of 0.1%. The hybrid nanofluids were characterized for their morphology using a transmission electron microscope. Hybrid nanofluid stability was monitored using UV visible spectrophotometer, viscosity, and visual inspection methods. The prepared nanofluids were observed to be stable with relatively constant viscosity and absorbance values. At 55 °C, maximum enhancements of 442.9% and 26.3%, and 288.0% and 19.3% were recorded for the electrical conductivity and viscosity of Al_2O_3–MWCNT/DIW nanofluids at particle mass ratios of 90:10 and 20:80, respectively, in relation to DIW. Temperature increase was observed to significantly reduce the viscosity of hybrid nanofluids while the particle mass ratio considerably and positively impacted the electrical conductivity. The relatively low viscosity of the hybrid nanofluids coupled with its reduction under increasing temperature and its insignificance increase as the particle mass ratio of the Al_2O_3 nanoparticles increased to make them viable coolants for engineering applications. New correlations were proposed to accurately estimate the viscosity and electrical conductivity of the hybrid nanofluids.

Keywords Al_2O_3 · MWCNT · Viscosity · Electrical conductivity · Coolant · Hybrid nanofluid

Abbreviations

Ag	Silver nanoparticles
Al_2O_3	Aluminum oxide nanoparticles
Au	Gold nanoparticles
C	Carbon
CNT	Carbon nanoparticle
Cu	Copper nanoparticles
CuO	Copper oxide nanoparticles

✉ Mohsen Sharifpur
mohsen.sharifpur@up.ac.za;
mohsensharifpur@duytan.edu.vn

1 Department of Mechanical and Aeronautical Engineering, University of Pretoria, Pretoria 0002, South Africa

2 Department of Mechanical Engineering, College of Engineering and Environmental Studies, Olabisi Onabanjo University, P.M.B. 2002, Ago-Iwoye, Nigeria

3 Institute of Research and Development, Duy Tan University, Da Nang 550000, Vietnam

4 Fluid Mechanics, Thermal Engineering and Multiphase Flow Research Lab. (FUTURE), Department of Mechanical Engineering, Faculty of Engineering, King Mongkut's University of Technology Thonburi (KMUTT), Bangkok 10140, Thailand

5 National Science and Technology Development Agency (NSTDA), Pathum Thani 12120, Thailand

6 School of Chemical Engineering and Technology, Xi'an Jiaotong University, Xi'an, China

7 Renewable Energy and Micro/Nano Sciences Lab., Department of Mechanical Engineering, Ferdowsi University of Mashhad, Mashhad, Iran

DIW	Deionized water
DW	Distilled water
EG	Ethylene glycol
EO	Engine oil
Fe_2O_3	Iron (III) oxide nanoparticles
GL	Glycerol
GO	Graphene oxide
h	Hour
ID	Inner diameter
L	Length
M	Mass (kg)
MgO	Magnesium oxide nanoparticles
MWCNT	Multiwalled carbon nanoparticle
ND	Nanodiamond
Ni	Nickel nanoparticles
OD	Outer diameter
PMR	Particle mass ratio
PWR	Particle mass ratio
PWR	Particle mass ratio
SDS	Sodium dodecyl sulfate
SiC	Silicon carbide
SiO_2	Silicon oxide nanoparticles
T	Temperature (°C)
TiO_2	Titanium oxide nanoparticles
W	Water
X	Percent mass ratio
Zn	Zinc nanoparticles
ZnO	Zinc oxide nanoparticles

Greek symbols

φ	Volume concentration (vol%)
μ	Viscosity (mPa s)
κ	Thermal conductivity (W m^{-1} K^{-1})
σ	Electrical conductivity (mS cm^{-1})
ρ	Density (g cm^{-3})

Subscripts

hnf	Hybrid nanofluid
nf	Nanofluid
bf	Base fluid
en	Enhancement
rel	Relative

Introduction

The nanosuspension termed "nanofluid" by Choi has drawn global attention to its inherent properties as a better thermal transporting medium in comparison with conventional working fluids. Pioneering and foremost studies on nanofluids have revealed the enhancements of the viscosity and thermal conductivity when compared with conventional base fluids (glycerol, ethylene glycol, water, and propylene glycol) [1–8]. In contemporary studies, other thermal properties such as $_{eff}$, σ_{eff}, $c_{p\text{-}eff}$, and dielectric apart from the κ_{eff} and μ_{eff} of nanofluids have been investigated in the literature [9–13]. In addition, several types of nanoparticles (Cu, MgO, CuO, CNT, SiO_2, ZnO, TiO_2, Al_2O_3, Fe_2O_3, Fe_3O_4, spinels, etc.) have been dispersed into diverse base fluids (water, ethylene glycol, engine oil, propylene glycol, bio-glycol, palm oil, glycerol, ionic fluid, coconut oil) for the experimental determination of their static thermophysical properties at various volume or mass concentrations for different temperature ranges [10–12, 14–18].

The concept of hybridization of nanoparticles has led to the synthesis of hybrid nanofluids known to be advanced thermal fluids with improved thermophysical properties. The pioneering work of Jana et al. [19] showed the preparation and κ_{eff} measurement of water-based mono-particle nanofluids (CNT, Cu, and Au) and hybrid nanofluids (CNT–Au/water and CNT–Cu/water). They found higher κ_{eff} for the mono-particle nanofluids than those of the hybrid nanofluids. Thereafter, numerous studies have been carried out on the experimental determination of the various thermal properties of hybrid nanosuspensions for different applications [20–32]. Suresh et al. [20] determined experimentally the μ_{eff} and κ_{eff} of water-based Al_2O_3–Cu (90%:10%) nanofluids ($\varphi = 0.1$–2%) prepared using two-step hydrogen reduction method with the aid of a surfactant. The μ_{eff} enhancement (8–115%) was noticed to be considerably more than that of κ_{eff} (1.47–12.11%) for the κ_{eff} range considered. Their result was the opposite of what was reported by Jana et al. [19] concerning the hybrid nanofluid κ_{eff} improvement.

Abbasi et al. [21] measured the κ_{eff} of water-based hybrid nanofluids of multi-walled CNT and gamma Al_2O_3 (1:1) for $\varphi = 0$–1%. The two-step method with a surfactant (Gum Arabic) was employed for the preparation. They revealed the augmentation of the κ_{eff} as the φ increased. A maximum enhancement of 20.68% at 1 vol% was recorded for the first functionalized sample. Using the same hybrid nanofluid (with the dispersion of equal solid volume of the nanoparticles of Al_2O_3 and MWCNT) and φ range as the work of Abbasi et al. [21] but at temperatures of 303, 314, 323 and 332 K, Esfe et al. [26] determined the κ_{eff} of the hybrid nanofluids. Their result showed that the κ_{eff} improvement of the nanofluids was a function of $\varphi\varphi$ and temperature.

In addition, the κ_{eff} and μ_{eff} of water-based hybrid nanofluids (Ag–MgO (50%:50%)) were measured experimentally for $\varphi = 0$–2% [33]. The μ_{eff} and κ_{eff} of the nanofluids were observed to enhance with an increase in φ. Also, Dardan et al. [34] examined the rheological behavior of Al_2O_3–MWCNT (75–25%)/EO nanofluid with φ range of 0–1%, temperatures of 25–50 °C and shear rates of 1333–13,333 s^{-1}. The results revealed the Newtonian nature of the hybrid nanofluids for the temperatures, φ and shear rates considered. The μ_{eff} was noticed to enhance with φ

and decreased as temperature increased. According to the sensitivity analysis carried out, the addition of the hybrid nanoparticles has more impact on the μ_{eff} than temperature. In comparison with EO, the highest μ_{eff} augmentation was 46% at 1.0 vol%. Furthermore, Kannaiyan et al. [35] investigated the ρ_{eff}, κ_{eff}, $c_{p\text{-}eff}$, and μ_{eff} of Al_2O_3–CuO/EG (80%)–water (20%) nanofluid for 0.05, 0.1, and 0.2 vol%, and temperatures of 20–70 °C. They found that all the measured thermophysical properties improved with an increase in φ. The μ_{eff} and κ_{eff} were observed to moderately reduced and increased with temperature, respectively, while $c_{p\text{-}eff}$ remained constant and density decreased slightly as temperature increased. Maximum κ_{eff} enhancement of 45% was achieved for the nanofluid.

Esfe and Sarlak [27] investigated the rheological behavior of MWCNT–CuO (15%:85%)/EO nanofluids with φ, shear rate, and temperature ranges of 0–1%, 2666.6–11,999.7 s^{-1}, and 5–55 °C, respectively. The hybrid nanofluids were found to exhibit non-Newtonian flow (Bingham pseudoplastic at < 45 °C and Bingham plastic > 45 °C) with highest μ_{eff} augmentation of 43.52% at 1 vol%. The μ_{eff} was noticed to enhance with an increase in φ and temperature due to the flow behavior of the hybrid nanofluid. Kakavandi and Akbari [28] also examined the influence of φ (0–0.75%) and temperature (25–50 °C) on the κ_{eff} of SiC–MWCNT (50%:50%)/water-EG (50%:50%) hybrid nanofluids. An enhancement of the κ_{eff} with an increase in temperature and φ was noticed. They recorded maximum κ_{eff} enhancement of 33%.

Akilu et al. [36] investigated the influence of increasing temperature (30–80 °C) and φ (0.5–2.0 vol%) on the $c_{p\text{-}eff}$, μ_{eff}, and κ_{eff} of SiO_2–CuO/C (80:20)/G-EG (60:40) nanofluids. In comparison with the G-EG, the μ_{eff} and κ_{eff} of the studied hybrid nanofluids were enhanced by 1.15-fold and 26.9%, respectively, while the $c_{p\text{-}eff}$ was reduced by 21.1% when $\varphi = 2.0$ vol% and at 80 °C. These properties were found to be improved compared with that of SiO_2/G-EG nanofluid (for example $\kappa_{eff} = 6.9\%$). Similarly, Rostami et al. [31] experimentally determined the κ_{eff} of CuO–GO (50:50)/W-EG (50:50 vol%) nanofluids at various $\varphi = 0.1$–1.6 vol% and temperatures (25–50 °C). Their results showed the highest improvement of 43.4% when $\varphi = 1.6$ vol% and at 50 °C. Rostami et al. [37] examined the influence of φ (0.1–1.6 vol%), temperatures (25–50 °C), and shear rates on the rheological behavior of CuO–GO (50:50)/W-EG (50:50 vol%) nanofluids. The hybrid nanofluids exhibited Newtonian behaviors when $\varphi \leq 0.4$ vol%, whereas pseudoplastic characteristics were observed when $\varphi > 0.4$ vol%. The μ_{eff} of the hybrid nanofluid was enhanced by 91.37% on increasing φ from 0.1 to 1.6 vol% at shear rate of 73.4 s^{-1} and temperature of 45 °C. Chereches and Minea [38] studied the σ_{eff} of Al_2O_3–SiO_2/water and Al_2O_3–TiO_2/water nanofluids at various temperatures (20–60 °C) and φ combinations (0.5:05, 0.5:1.0, and 0.5:1.5 (Al_2O_3:SiO_2/TiO_2)). They reported that σ_{eff} was augmented by 14–40-fold and 30–58-fold for SiO_2/water and TiO_2/water nanofluids, respectively, in comparison with water, at 60 °C and highest φ combination. With TiO_2/water nanofluids possessing higher σ_{eff} than SiO_2/water nanofluids, maximum enhancement of σ_{eff} of Al_2O_3–TiO_2/water nanofluids was 43–57-fold, when compared with water.

The influence of variation in shear rate, temperature (25–50 °C), and φ (0.25–2 vol%) on the rheological behavior of TiO_2–MWCNT (80:20)/EO nanofluids was examined by Alarifi et al. [39]. The authors demonstrated that under the studied conditions, Newtonian behaviors were displayed by the hybrid nanofluids. The highest enhancement of μ_{eff} by 42% with $\varphi\varphi = 2$ vol% and 50 °C was reported. Gangadevi and Vinayagam [40] measured the κ_{eff} and μ_{eff} of Al_2O_3–CuO (50:50)/DW nanofluids under increasing temperature (20–60 °C) and φ (0.05–0.2 vol%). Results revealed that μ_{eff} of the hybrid nanofluids was augmented by 2–11% when compared with that of CuO/DW nanofluids at the temperature range of 20–60 °C. Lowest μ_{eff} was observed for Al_2O_3/DW nanofluids relative to Al_2O_3-CuO (50:50)/DW and CuO/water nanofluids. At 60 °C and $\varphi = 0.2$ vol%, the κ_{eff} of Al_2O_3-CuO (50:50)/DW, CuO/DW, and Al_2O_3/DW nanofluids was augmented by 21%, 12.15%, and 11.23%, respectively, when compared with DW. Also, the impact of temperature (5–55 °C), shear rate (660.5–13,300 s^{-1}), and volume fraction (0.05%–0.8%) on the μ_{eff} of ZnO–MWCNT (75:25)/EO nanofluids was examined by Goordarzi et al. [41]. They reported that at the studied temperature, shear rate, and φ, the hybrid nanofluids displayed Newtonian behaviors. However, at lower temperatures and higher φ, a pseudoplastic behavior was exhibited by the hybrid nanofluids.

Subject to the above literature, it can be noticed that the measured thermal properties (mainly κ_{eff} and μ_{eff}) of hybrid nanofluids were studied at a fixed particle mixing ratio with the variation of parameters such as temperature, φ, and shear rate. However, current progress in research has revealed the measurement of thermal properties of hybrid nanofluids at different particle mixing ratios to better understand which particle mixing ratio afforded the highest value of thermal properties. Mechiri et al. [42] studied the influence of PMRs (75:25, 50:50, and 25:50), temperatures (30–60 °C) and φ (0.1–0.5 vol%) on the μ_{eff} and κ_{eff} of groundnut-based Cu–Zn nanofluids. They reported that the Cu–Zn (50:50)/groundnut nanofluids have the highest κ_{eff} and μ_{eff} and were considered to be the best fluids. Changes in temperature and φ were observed to affect κ_{eff} and μ_{eff} more than PMR. Newtonian behavior was displayed by both the groundnut and hybrid nanofluids. The effect of five different mixing ratios (20:80–80:20) and temperatures (30–80 °C) on the κ_{eff} and μ_{eff} of W-EG (60:40)-based TiO_2–SiO_2 nanofluids formulated at $\varphi = 1.0$ vol% was examined by Hamid et al. [43].

The maximum κ_{eff} enhancement of 16% was reported for TiO_2–SiO_2/W-EG nanofluid with a mixing ratio of 20:80 compared with W-EG while the highest value of μ_{eff} was recorded for TiO_2–SiO_2 (40–60)/W-EG nanofluid. Owing to these results, the fluids with mixing ratios of 40:60 and 80:20 were considered as the best hybrid nanofluids for thermal cooling purposes. However, the hybrid nanofluid with a mixing ratio of 50:50 was noticed to be the poorest as a coolant as it possessed the lowest κ_{eff} and the highest μ_{eff}.

The influence of PMRs (70:30, 50:50, and 30:70), temperatures (25–40 °C), and φ (0.005–0.1 vol%) on the κ_{eff} of Al_2O_3-Ag/DW nanofluids was studied by Aparna et al. [44]. The result proved that the maximum κ_{eff} was obtained with Al_2O_3–Ag (50–50)/DW nanofluids. The κ_{eff} of Al_2O_3–Ag/DW nanofluids was above that of Al_2O_3/DW nanofluids with Ag/DW nanofluids having the highest value as Ag nanoparticles have higher κ_{eff} than Al_2O_3 nanoparticles. Recently, Wole–sho [45] studied the κ_{eff} of Al_2O_3–Zn/DW nanofluids under changing PMRs (1:2, 1:1, and 2:1), temperatures (25–40 °C), and φ (0.33–1.67 vol%). They showed that maximum κ_{eff} enhancements for Al_2O_3–Zn/DW nanofluids with PMRs of 1:1, 1:2, and 2:1 were 35%, 36%, and 40%, respectively, in comparison with DW at 40 °C and $\varphi = 1.67$ vol%. A summary of the literature review on the thermal properties of hybrid nanofluids is provided in Table 1 for better understanding.

This present study was conducted in furtherance to the above trend of research and to contribute to the body of knowledge in documenting the effect of variation in PMR on the thermal properties of hybrid nanofluids. To the best of the authors' knowledge, the μ_{eff} and σ_{eff} of Al_2O_3–MWCNT/DIW nanofluid have not been studied before now and this work aimed at examining the influence of PMRs (90:10, 80:20, 60:40, 40:60, and 20:80) on the μ_{eff} and σ_{eff} at $\varphi = 0.1$ vol% under increasing temperature (15–55 °C). The open literature has shown that the MWCNT and Al_2O_3 nanoparticles are the most used (on an individual basis) to prepare nanofluids due to their stability in different base fluids. Also, MWCNT nanoparticles are expensive while Al_2O_3 nanoparticles are comparatively cheaper and thus employing both in this study by hybridizing them at different PMRs.

Experimental

Materials and equipment

Nanoparticles of γ-Al_2O_3 with 20–30 nm diameter (as specified by the manufacturer) were sourced from Nanostructured and Amorphous Materials Inc., Houston, Texas, USA. Functionalized MWCNT nanoparticles with lengths, inner and outer diameters of 10–30 µm, 3–5 nm, and 10–20 nm, respectively, were purchased from MKnano Company, Ontario, Canada. Sodium dodecyl sulfate (SDS) with a purity of ≥ 98.5% bought from Sigma-Aldrich, Germany, was used as a surfactant. An ultrasonicator (Hielscher UP200S (Germany); 400 W and 50 Hz) was used to homogenize the hybrid nanoparticles (MWCNT and γ-Al_2O_3) and DIW mixture while a programmable water bath (LAUDA ECO RE1225) was used to attain the desired temperature in this work. Other equipments used were; UV–visible spectrophotometer (Jenway; model 7315), pH meter (Jenway 3510; −2 to 19.999 range and ± 0.003 accuracy), electrical conductivity meter (EUTECH Instrument (CON700); ± 1% accuracy), digital weighing balance (Radwag AS 220.R2 (Poland) with a measurement range of 10 mg–220 g and accuracy of ± 0.01 g), transmission electron microscope (TEM) (JEOL JEM-2100F), and vibro-viscometer (SV-10, A&D, Japan, ± 1% accuracy).

Hybrid nanofluid preparation and stability

A two-step method was used in the formulation of the hybrid nanofluids. The amount of SDS used for the preparation of hybrid nanofluids was calculated based on a dispersion fraction of 1.0. With 80 mL of DIW and $\varphi = 0.1$ vol%, Eq. (1) was used to estimate the masses of individual nanoparticles deployed to prepare the hybrid nanofluids. The estimated amounts of SDS, Al_2O_3, and MWCNT nanoparticles based on the studied PMRs of 90:10, 80:20, 60:40, 40:60, and 20:80 and $\varphi = 0.1$ vol% were dispersed into DIW. The choice of $\varphi = 0.1$ vol% was informed by the knowledge that maximum heat transfer and Nusselt number were attained at this value in previous studies on the natural convection of water-based Al_2O_3 and MWCNT nanofluids in square cavities [46–50]. The mixture was homogenized by sonicating it for 2 h at an amplitude of 75% and a frequency of 70% with the aid of an ultrasonicator. While sonicating, the mixture was immersed in a water bath and maintained at a constant temperature (20 °C). The morphology of the hybrid nanoparticles in the Al_2O_3–MWCNT (80:20)/DIW nanofluids was monitored using TEM while the stability of hybrid nanofluids with PMRs of 90:10 and 80:20 was checked using μ and UV–visible methods. The visual technique was used to monitor the stability of all the hybrid nanofluid samples. Both the μ and UV–visible techniques were conducted for 24 h while the visual method was engaged weekly for a month.

$$\varphi = \left(\frac{X_{Al_2O_3}\left(\frac{M}{\rho}\right)_{Al_2O_3} + X_{MWCNT}\left(\frac{M}{\rho}\right)_{MWCNT}}{X_{Al_2O_3}\left(\frac{M}{\rho}\right)_{Al_2O_3} + X_{MWCNT}\left(\frac{M}{\rho}\right)_{MWCNT} + \left(\frac{M}{\rho}\right)_{water}} \right). \tag{1}$$

Table 1 Summary of studies on the thermal properties of hybrid nanofluids

Author	HNPs/ratio	Mixing ratio	Base fluid	Properties	Temperature	φ/vol%	Enhancement/%
Jana et al. [17]	Au, CNT, Cu, CNT–Cu and CNT–Au	1.5–2.5	DIW	κ_{eff}	Room temp	0.3 and 0.5 (CNT) 1.4 (Au) and 0.05–0.3 (Cu)	74 (Cu)
Kannaiyan et al. [33]	Al_2O_3–CuO	–	DIW-EG (80:20)	ρ_{eff}, μ_{eff}, & ρ_{eff}	20–60	0.05–0.2	45
Esfe et al. [24]	Ag–MgO	50:50	DW	κ_{eff} and μ_{eff}	Room temp	0–2	–
Abbasi et al. [19]	MWCNT–Al_2O_3	1:1	DIW	κ_{eff}	Room temp	0.1	20.68
Akilu et al. [34]	SiO_2–CuO/C	80:20	GL-EG (60:40 mass%)	$C_{p\text{-}eff}$, κ_{eff}, and μ_{eff}	30–80	0.5–2.0	1.15X (μ_{eff}); 21.1 ($C_{p\text{-}eff}$); 26.9 (κ_{eff})
Kakavandi and Akbari [26]	MWCNT–SiC	50:50	W-EG (50:50 vol%)	κ_{eff}	25–50	0.05–0.75	33%
Suresh et al. [18]	Al_2O_3–Cu	90:10	DIW	κ_{eff} and μ_{eff}	Room temp	0.1–2.0	1.47–12.11 (κ_{eff}); 8–115 (μ)
Asadi et al. [27]	Al_2O_3–MWNCT	–	Thermal oil	κ_{eff} and μ_{eff}	25–50	0.125–1.5	45% (κ_{eff}) and 81% (μ_{eff})
Esfe et al. [24]	CNT–Al_2O_3	–	W	κ_{eff}	30–60	0.02–1.0	–
Esfe and Sarlak [25]	CuO–MWCNT	85:15	EO	μ_{eff}	5–55	0.05–1.0	43.52%
Chereches and Minea	Al_2O_3–TiO_2 and Al_2O_3–SiO_2	–	W	σ_{eff}	20–60	0.05:0.05–1.5	σ_{eff} of Al_2O_3-TiO_2 nanofluids > Al_2O_3–SiO_2 nanofluids
Goodarzi et al. [39]	ZnO–MWCNT	75:25	EO	μ_{eff}	5–55	0.05–0.8	20% (at 5 °C and 0.8 vol%)
Gangadevi and Vinayagam [38]	Al_2O_3–CuO	50:50	DW	κ_{eff} and μ_{eff}	20–60	0.05–0.2	κ_{eff} = 21% and μ_{eff} = 13% (for 0.2 vol%)
Alarifi et al. [37]	MWCNT–TiO_2	80:20	EO	μ_{eff}	25–50	0.25–2.0	42% (2.0 vol%)
Giwa et al. [62]	Al_2O_3–Fe_2O_3	25:75	DIW	κ_{eff} and μ_{eff}	20–40	0.05–0.3	μ_{eff} = 4.55–20.43% and κ_{eff} = 0.58%–3.32%
Giwa et al. [58]	Al_2O_3–Fe_2O_3	25:75	DIW and EG-DIW (40:60 vol%)	σ_{eff} and μ_{eff}	20–50	0.05–0.75	DW (μ_{eff} = 43.64% and σ_{eff} = 1692.16%) and EG-DW (μ_{eff} = 49.38% and σ_{eff} = 7618.89%)
Mechiri et al.	Cu–Zn	75:25, 50:50, 25:75	Groundnut	κ_{eff} and μ_{eff}	30–60	0.1–0.5	Cu–Zn (50:50) with highest κ_{eff} value.
Wole-Osho et al.	Al_2O_3–ZnO	1:2, 1:1, 2:1	DW	κ_{eff}	25–65	0.33–1.67	Maximum κ_{eff} was 35% (1:1), 36% (1:2), & 40% (2:1)
Hamid et al. [41]	TiO_2–SiO_2	20:80–80:20	W-EG (60:40 vol%)	κ_{eff} and μ_{eff}	30–80	0.1	Maximum κ_{eff} = 16%. Best hybrid nanofluids are 40:60 and 60:20
Aparna et al. [42]	Al_2O_3–Ag	50:50; 30:70; 70:30	DW	κ_{eff}	25–52	0.005–0.1	23.82%

Electrical conductivity and pH measurements

The electrical conductivity meter was calibrated using the standard calibration fluid supplied by the manufacturer. The glycerine (standard fluid) was measured at 25 °C in triplicate, and the average (1414 μScm^{-1}) was reported. This was found to be close to the glycerine value of 1413 μScm^{-1} (at 25 °C) provided by the manufacturer. Thereafter, the σ of DIW and hybrid nanofluids was measured at 15–55 °C. The uncertainty related to the measurement of σ was estimated to be 1.85%. The sources of error were from the weighing of surfactant, MWCNT, and Al_2O_3 nanoparticles, and σ measurement. A 3-point calibration of the pH meter was carried out using buffer solutions (as standard fluids) with a pH of 4, 7, and 10 at room temperature before the measurement of σ of DIW and hybrid nanofluids. With sources of error emanating from the weighing balance (due to measurement of SDS, MWCNT, and Al_2O_3 nanoparticles) and pH meter (temperature and pH measurement), the uncertainty of 3.4% was estimated. The σ_{rel} and σ_{en} of the hybrid nanofluids were determined using Eqs. 2 and 3, respectively.

$$\sigma_{\text{rel}} = \frac{\sigma_{\text{hnf}}}{\sigma_{\text{bf}}} \tag{2}$$

$$\sigma_{\text{en}}(\%) = \left(\frac{\sigma_{\text{hnf}} - \sigma_{\text{bf}}}{\sigma_{\text{bf}}} \right) \times 100. \tag{3}$$

Viscosity measurement

The viscometer was engaged in the measurement of the μ of DIW and hybrid nanofluids at temperatures of 15–55 °C. Prior to the measurement, the viscometer was calibrated using DIW. The reliability of the viscometer was carried out by measuring the μ of DIW at the predetermined temperatures (15–55 °C) and comparing the same with standard values of water reported in the literature [51]. The uncertainty associated with the measured μ was 2.05%. Errors from the weighing balance (for determining the mass of surfactant, MWCNT, and Al_2O_3 nanoparticles) and viscometer (temperature and μ data) were propagated for evaluating the uncertainty. Figure 1 shows the experimental setup of this study. The μ_{rel} and μ_{en} of the hybrid nanofluids in relation to the DIW were estimated by Eqs. 4 and 5, respectively.

$$\mu_{\text{rel}} = \frac{\mu_{\text{hnf}}}{\mu_{\text{bf}}} \tag{4}$$

$$\mu_{\text{en}}(\%) = \left(\frac{\mu_{\text{hnf}} - \mu_{\text{bf}}}{\mu_{\text{bf}}} \right) \times 100 \tag{5}$$

Fig. 1 Experimental set-up for viscosity and electrical conductivity

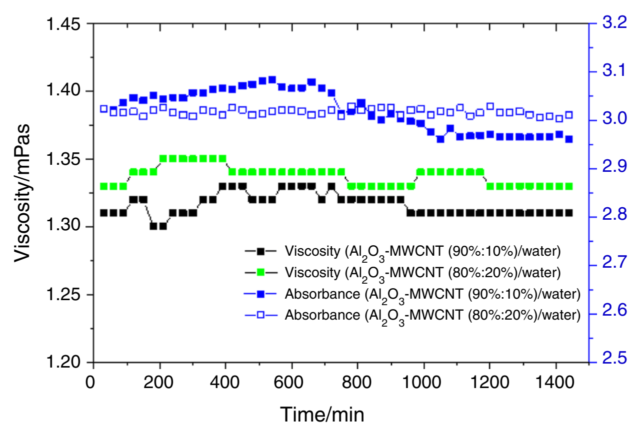

Fig. 2 Stability of hybrid nanofluids (with particle mass ratios of 90:10 and 80:20) using viscosity and absorbance

It is worth mentioning that the duration of the experiment from the preparation of hybrid nanofluid at a certain PMR to the measurement of the thermal properties (μ and κ) took an average of 8 h.

Results and discussion

Al_2O_3–MWCNT/water nanofluid stability

In this work, the stability of the formulated hybrid nanofluids was monitored using a UV–visible spectrophotometer, μ, and visual inspection methods. Figure 2 shows the stability of the hybrid nanofluids (Al_2O_3–MWCNT/DIW with PMRs of 90:10 and 80:20) via μ (at 20 °C) and absorbance of 3 at a maximum wavelength of 261 nm. The relatively straight lines (horizontal) of the μ and absorbance indicated that the nanofluids were stable for 24 h which was longer than the 6 h (maximum) required for measuring the studied thermal properties. The absorbance of the other three nanofluids was observed to be around 3 at a wavelength range of 261–301 nm. Solomon et al. [52] and Ghodsinezhad et al. [46] reported absorbance of 3 and wavelength of 225 nm, respectively, for Al_2O_3/DIW nanofluids, which was in close agreement with the values recorded in this present work. The addition of the MWCNT nanoparticles into DIW was noticed to cause the shift in wavelength, of which wavelength of about 240 nm was determined for MWCNT/water nanofluid [53]. The visual method showed no sedimentation of the hybrid nanofluids for a month (see Fig. 3).

Figure 4 shows the TEM image of Al_2O_3–MWCNT (80:20)/DIW nanofluids. The rod-like images indicated the presence of the MWCNT nanoparticles, while the spherical-shaped images revealed the existence of Al_2O_3 nanoparticles. As detected by the TEM, a good dispersion of the Al_2O_3 nanoparticles into the surface of the MWCNT nanoparticles is noticed in Fig. 4, thus confirming the stability of the hybrid nanofluid.

pH and electrical conductivity of hybrid nanofluids

The obtained range of pH values for the studied hybrid nanofluids was 6.1–8.7. The pH ranges of 7–8.2 and 7.5–8.5, and 6.2–6.8 were reported in the literature for Al_2O_3 and Al_2O_3–CuO water-based nanofluids, which were in close range to that measured in this work [54, 55]. The capability of an aqueous solution to conduct electric current is the electrical conductivity. It is one of the thermophysical properties of nanofluids and can be used as an indicator to monitor the stability of nanofluids. The electrical conductivity of mono-particle and hybrid nanofluids is a rarely studied property. The dispersion of nanoparticles into a base fluid is known to introduce electric charges into the aqueous solution due to the Brownian motion of charged ions from the nanoparticles. This leads to the formation of an electric double layer around the nanoparticles which makes the resulting aqueous solution to be electric conducting when an electric potential is applied across.

Figure 5 depicts the σ of DIW and Al_2O_3–MWCNT/DIW nanofluids against the PMRs under increasing temperature

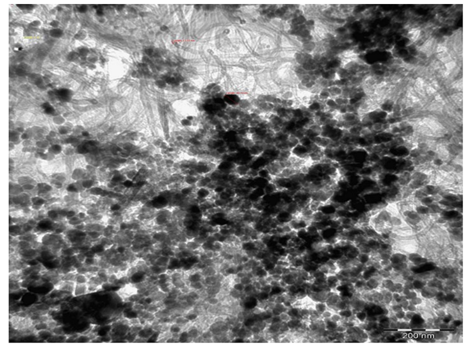

Fig. 4 Morphology of the Al_2O_3–MWCNT (80:20)/DIW nanofluids using TEM

Fig. 3 Visual stability of the hybrid nanofluids

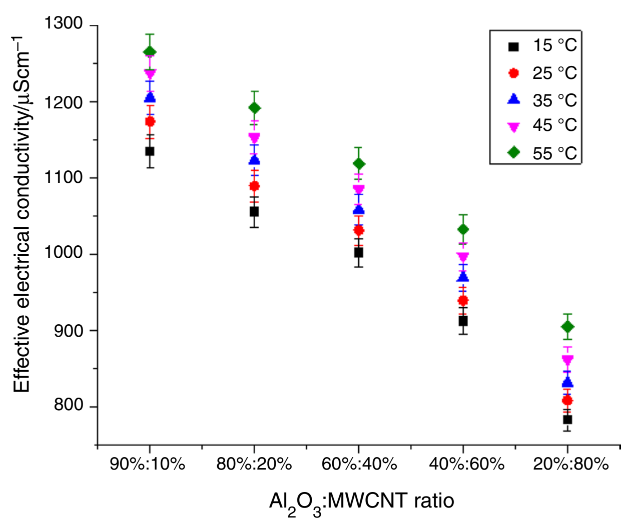

Fig. 5 Effective electrical conductivity of hybrid nanofluids against particle mass ratios under increasing temperature

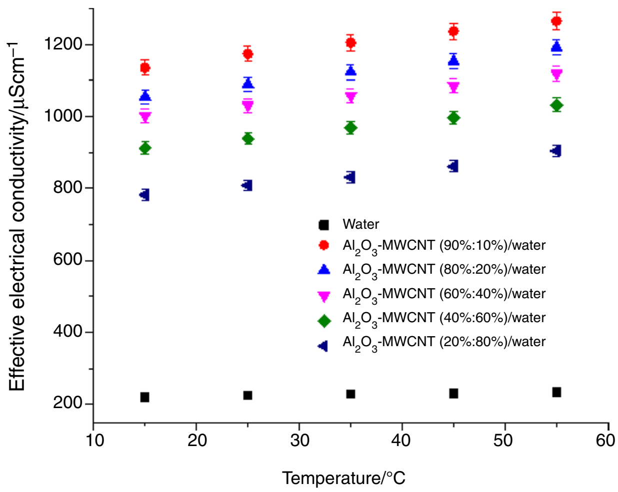

Fig. 6 Effective electrical conductivity of hybrid nanofluids against temperature at different particle mass ratios

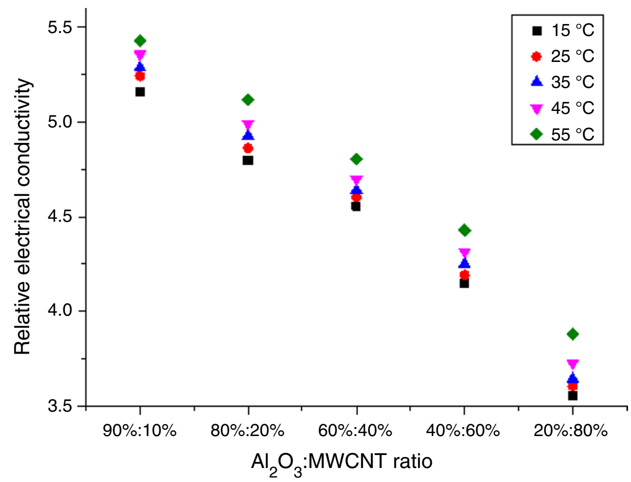

Fig. 7 Relative electrical conductivity of hybrid nanofluids against particle mass ratios under increasing temperature

(15–55 °C). The addition of the hybrid nanoparticles into DIW resulted in an appreciable augmentation of the σ of DIW. It can be noticed in Fig. 5 that as the PMR of Al_2O_3 nanoparticles increased, the σ_{eff} was significantly enhanced, whereas the reverse was observed when the PMR of MWCNT nanoparticles increased. This observation can be strongly linked to the σ of Al_2O_3 and MWCNT nanoparticles of which Al_2O_3 nanoparticles have a higher value. Thus, increasing the PMR of Al_2O_3 nanoparticles in the hybrid nanofluid would enhance σ_{eff}. As shown in Fig. 6, increasing the temperature of the hybrid nanofluid at varying PMRs was observed to slightly enhance σ_{eff}. With the studied PMRs temperatures, a range of 789–1265 μScm^{-1} was measured for the σ_{eff} of Al_2O_3–MWCNT/DIW nanofluids. The maximum value of 1265 μScm^{-1} was recorded for the hybrid nanofluid with PMR of 90:10 t 55 °C, as it contained the highest PMR of Al_2O_3 nanoparticles. This finding is evident in Figs. 5 and 6. At 55 °C, increasing the PMR of MWCNT nanoparticles from 10 to 80 was observed to reduce the σ_{eff} from 1265 μScm^{-1} to 904 μScm^{-1}.

The effect of PMR on the σ_{eff} was found to be significant compared with that of temperature as presented in Figs. 5 and 6, respectively. It can be discussed that the addition of hybrid nanoparticles (at various PMRs) to DIW resulted in increased presence, quantity, and mobility of charged ions in DIW. This also led to an increase in the formation of an electric double layer and increment in the size of the electric double layer; thus, a considerable measure of σ_{eff} was recorded. However, the increase in temperature only slightly increased the mobility of the charged ions due to Brownian motion, thereby slightly augmenting σ_{eff}.

However, Zawrah et al. [55] measured σ_{eff} of Al_2O_3/water nanofluid ($\varphi = 0.2$ vol% and at 25.9 °C) as 2370 μScm^{-1}. The hybridization of the Al_2O_3 nanoparticles with MWCNT nanoparticles may be responsible for the reduction in the value of σ_{eff} obtained in this work compared to that of Zawrah et al. [55]. The results obtained in this present study were consistent with previous studies in which the σ_{eff} of mono-particle nanofluids improved as temperature and φ increased [38, 53, 56, 57].

Figure 7 presents the σ_{rel} of Al_2O_3–MWCNT/DIW nanofluid as related to PMR under changing temperature. The σ_{rel} of the hybrid nanofluids was found to enhance with an increase in the PMR of Al_2O_3 nanoparticles and detracted with increasing PMR of MWCNT nanoparticles in comparison with DIW. It was also noticed that as the temperature increased, the σ_{rel} increased. At 55 °C, the highest σ_{rel} was 5.4 for Al_2O_3–MWCNT (90:10)/DIW nanofluid while the lowest was 3.88 for Al_2O_3–MWCNT (20:80)/DIW nanofluid.

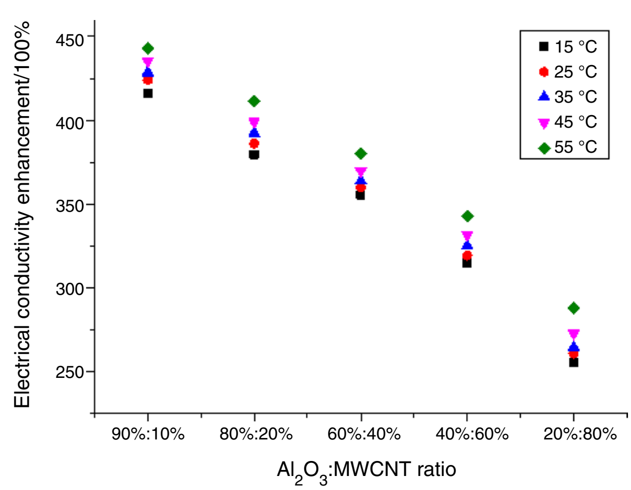

Fig. 8 Electrical conductivity enhancement of hybrid nanofluids against particle mass ratios at different temperatures

The σ_{en} of Al_2O_3–MWCNT/DIW nanofluid against PMRs under increasing temperature is presented in Fig. 8. The σ_{en} of the hybrid nanofluids was observed to be related to the temperature and PMR. Maximum enhancements (σ_{en}) of 443% and 288% were achieved for Al_2O_3–MWCNT/DIW nanofluids with PMRs of 90:10 and 20:80, respectively, at 55 °C, in comparison with DIW. A range of 255–443% was recorded for σ_{en} of Al_2O_3–MWCNT/DIW nanofluid at the PMRs and temperatures considered in this study. It was obvious that the σ_{en} was drastically reduced with a high PMR of MWCNT nanoparticles.

With the use of mono-particle nanofluids, σ_{en} was augmented by 2127% [58], 5112% [57], 190.57% [53], 855% [11], and 2370% [55] for Al_2O_3/water (at $\varphi = 0.5$ vol% and 45 °C), Al_2O_3/Bio-glycol ($\varphi = 0.1$ vol%), MWCNT/solar glycol (at $\varphi = 0.6$ vol% and 50 °C), MWCNT/water (at $\varphi = 0.5$ vol% and 23 °C), and Al_2O_3/water (at $\varphi = 2$ vol% and 25.9 °C) nanofluids, in comparison with the respective base fluids. These published values showed that the obtained result in this present work was well within the values reported in the literature. The influence of φ and temperature on the σ_{en} was also emphasized by the previous studies. Similarly, previous studies on the σ_{en} of hybrid nanofluids revealed 1339.81%–853.15% [59], 163.37–1692.16% [60], 97–557% [61], and 43-fold–57-fold for ND-Ni (85:15)/DW ($\varphi = 0.1$ vol% and 24–65 °C), Fe_2O_3-Al_2O_3 (75:25)/DIW ($\varphi = 0.05$–0.75 vol% and 20–50 °C), SiO_2-G/naphthenic mineral oil ($\varphi = 0.01$–0.08 mass% and room temperature), and Al_2O_3 (0.5 vol%)–SiO_2 (1.5 vol%) (20–60 °C) nanofluids, respectively, which closely agreed with the results obtained in this study. The disparity in σ_{en} can be linked to the variation in φ, temperature, and types of hybrid nanoparticles used to prepare hybrid nanofluids.

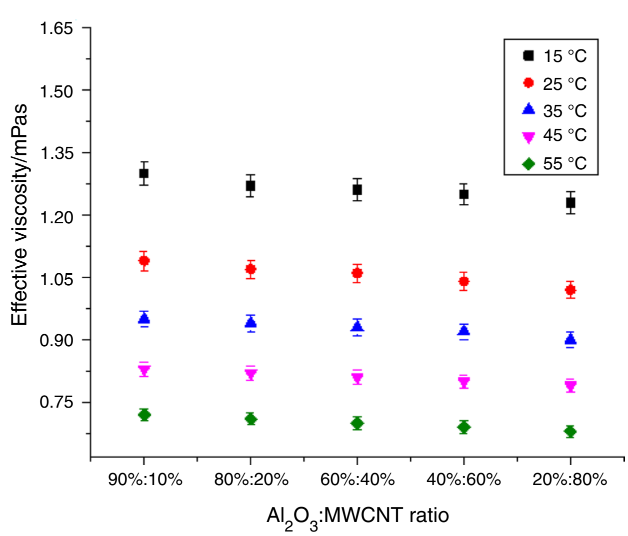

Fig. 9 Effective viscosity of hybrid nanofluids against particle mass ratios under increasing temperature

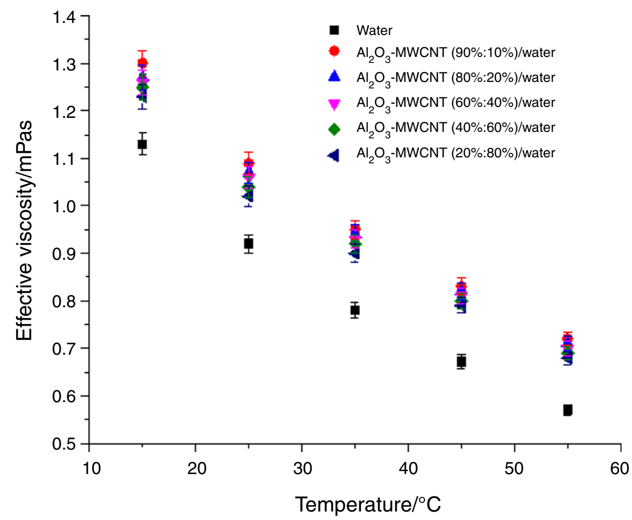

Fig. 10 Effective viscosity of hybrid nanofluids against temperature at different particle mass ratios

Viscosity of hybrid nanofluids

The μ_{eff} of Al_2O_3–MWCNT/DIW nanofluids against PMR at varying temperatures is presented in Fig. 9. Increasing PMR of Al_2O_3 nanoparticles was observed to slightly enhance μ_{eff} of Al_2O_3–MWCNT/DIW nanofluid, whereas the reverse was noticed when the PMR of MWCNT nanoparticles was increased. From Fig. 10, the hybrid nanofluids and DIW displayed a decaying trend of μ_{eff} with a temperature rise. The μ_{eff} of all the hybrid nanofluid samples was found to be higher than that of DIW. At 15 °C, the μ_{eff} decreased from 1.30 mPas to 1.23 mPas when the PMR of MWCNT nanoparticles increased from 10 to 80 whereas at 15 °C, μ_{eff} reduced from 0.72 mPas to 0.68 mPas. It can be deduced that an increase in temperature has a significant impact on the μ_{eff} (also see Fig. 10). This agreed with previous studies on the μ_{eff} of mono-particle and hybrid nanofluids [29, 34, 43, 62].

It can be observed that the dispersion of hybrid nanoparticles (at various PMRs) into DIW generally enhanced the μ of DIW. This can be attributed to the higher density of MWCNT and Al_2O_3 nanoparticles compared with DIW (see Table 1). The presence of the hybrid nanoparticles increased the intermolecular forces between particle–particle and particle–water, and also reduced the collision of DIW molecules due to the existence of Brownian motion, thus increasing the flow resistance of the hybrid nanofluid. Under increasing temperature, the intermolecular forces are weakened coupled with increased agitation of molecules (particle–particle and particle–water) due to Brownian motion, thus leading to a reduction in flow resistance and, thus, better flow of hybrid nanofluids.

Using Eq. 4, the μ_{rel} of the hybrid nanofluids was evaluated and is presented in Fig. 11 as a function of PMR with

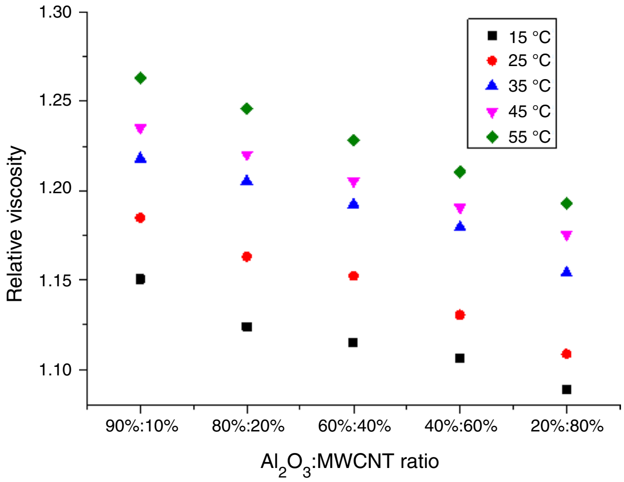

Fig. 11 Effective viscosity of hybrid nanofluids against particle mass ratios under increasing temperature

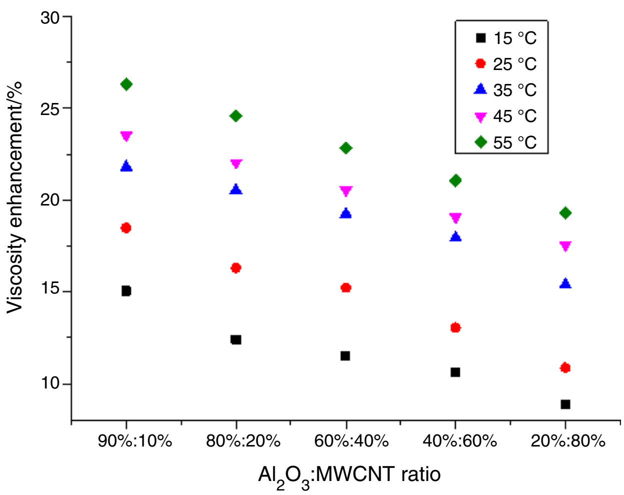

Fig. 12 Viscosity enhancement of hybrid nanofluids against particle mass ratios at different temperatures

increasing temperature. The μ_{rel} was observed to augment with an increase in PMR of Al_2O_3 nanoparticles and detracted with a temperature rise for all the hybrid nanofluids, which was in agreement with the earlier studies [62, 63]. However, the work of Dardan et al. [34] demonstrated the opposite of the trend noticed in this study as the μ_{rel} of Al_2O_3–MWCNT/EO nanofluid reduced with temperature. Minimum μ_{rel} of 1.09 was noticed for Al_2O_3–MWCNT/DIW nanofluid with PMR of 20:80 at 15 °C while the Al_2O_3–MWCNT/DIW nanofluid with PMR of 90:10 has maximum μ_{rel} (1.26) at the temperature of 55 °C.

The μ_{en} afforded by the hybrid nanofluids when compared with DIW in terms of the PMR and temperature is shown in Fig. 12. The μ_{en} of the hybrid nanofluids was attenuated as the PMR of MWCNT nanoparticles increased in comparison with DIW. In addition, the rise in temperature contributed to an increase in μ_{en} relative to DIW, which was found to be consistent with previous studies [36, 60, 62, 64]. At 55 °C, the highest and lowest μ_{en} were 26.3% and 19.3% for Al_2O_3–MWCNT/DIW nanofluid with PMR of 90:10 and 20:80, respectively, in comparison with DIW, respectively. This translated to a 7% reduction of μ_{en} as the PMR of MWCNT nanoparticles increased from 10 to 80.

Previous studies on the μ_{en} of hybrid nanofluids reported 23.24% ($\varphi = 0.3$ vol% and 60 °C) [65], 1.5-fold ($\varphi = 0.3$ vol% and 60 °C) [66], 8–11% ($\varphi = 0.1$–2.0 vol% and room temperature) [20] and 4.55%–20.43% ($\varphi = 0.05$–0.3 vol% and 20–60 °C) [64] for ND-Ni (84:16), CNT–Fe_3O_4 (26:74), Al_2O_3–Cu (90:10), and Al_2O_3–Fe_2O_3 (25:75) DIW-based nanofluids, respectively, which agreed with the results obtained in this present study. For mono-particle nanofluids, μ_{en} of 30%, 70%, and 58% have been published in the literature [48] for Al_2O_3 (3.0 vol%; 21–39 °C), MWCNT (0.2 vol%; 5–65 °C) and MWCNT (1.0 vol%; 27 °C) water-based nanofluids compared with DIW, which were higher than the range of values measured in this work. It is therefore apparent that the hybridization of MWCNT and Al_2O_3 nanoparticles caused a reduction in the μ_{eff}, especially at higher PMR of MWCNT nanoparticles, which is beneficial for the utilization of Al_2O_3–MWCNT/DIW nanofluids as thermal media for engineering applications as pumping power and frictional losses would be reduced thereby increasing overall thermal efficiency [11, 67].

In addition, Hamid et al. [43] and Mechiri et al. [42] showed that by varying the PMRs of TiO_2–SiO_2/W-EG (20:80–80:20) and Cu–Zn/groundnut (75:25, 50:50, and 25:50) nanofluids, the lowest and highest μ_{eff} values were achieved at PMRs of 80:20 and 50:50, and 75:25 and 50:50, respectively. Considering the result of this present study that minimum and maximum μ_{eff} were attained at PMRs of 20:80 and 90:20, respectively, it showed that probably no general optimum PMR existed for the μ_{eff} of hybrid nanofluids.

Table 2 Properties of MWCNT and Al_2O_3 used in this work

Property	MWCNT	Al_2O_3
Purity (%)	> 97	99.97
Size (nm)	$L = 10$–30 nm; OD = 10–20 nm; ID = 3–5 nm	20–30
Color	Black	White
Thermal conductivity/Wm^{-1} k^{-1}	3000	40
True density/g cm^{-3}	2.1	3.97
Specific surface area/m^2 g^{-1}	233	180

Table 3 Developed correlations for the Al_2O_3–MWCNT nanofluids

Ratio	Effective electrical conductivity	Effective viscosity
90:10	$\frac{\sigma_{hnf}}{\sigma_{bf}} = 5.0650 + 0.00654T$ $R = 0.997$; $R^2 = 0.991$	$\frac{\mu_{hnf}}{\mu_{bf}} = 1.06175 + 0.00753T - 1.26 \times 10^{-4}T^2 + 1.00 \times 10^{-6}T^3$ $R = 0.998$; $R^2 = 0.987$
80:20	$\frac{\sigma_{hnf}}{\sigma_{bf}} = 4.6682 + 0.00771T$ $R = 0.988$; $R^2 = 0.969$	$\frac{\mu_{hnf}}{\mu_{bf}} = 1.02752 + 0.00777T - 1.03 \times 10^{-4}T^2 + 6.11 \times 10^{-7}T^3$ $R = 0.997$; $R^2 = 0.972$
60:40	$\frac{\sigma_{hnf}}{\sigma_{bf}} = 4.4528 + 0.0059T$ $R = 0.977$; $R^2 = 0.940$	$\frac{\mu_{hnf}}{\mu_{bf}} = 1.02273 + 0.00744T - 9.82 \times 10^{-5}T^2 + 5.55 \times 10^{-7}T^3$ $R = 0.996$; $R^2 = 0.968$
40:60	$\frac{\sigma_{hnf}}{\sigma_{bf}} = 4.0245 + 0.00692T$ $R = 0.984$; $R^2 = 0.957$	$\frac{\mu_{hnf}}{\mu_{bf}} = 1.0760 + 6.32 \times 10^{-4}T + 1.05 \times 10^{-4}T^2 - 1.31 \times 10^{-6}T^3$ $R = 0.989$; $R^2 = 0.909$
20:80	$\frac{\sigma_{hnf}}{\sigma_{bf}} = 3.4130 + 0.00771T$ $R = 0.960$; $R^2 = 0.920$	$\frac{\mu_{hnf}}{\mu_{bf}} = 1.10178 - 0.00394T + 2.36 \times 10^{-4}T^2 - 2.44 \times 10^{-6}T^3$ $R = 0.996$; $R^2 = 0.967$

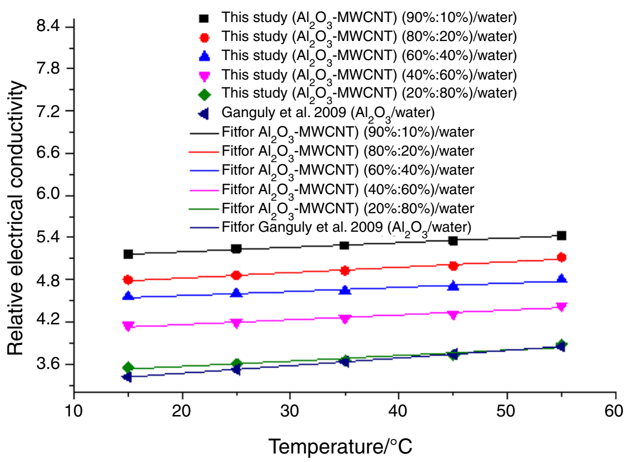

Fig. 13 Comparison of developed correlations (electrical conductivity) to an existing correlation at different temperatures

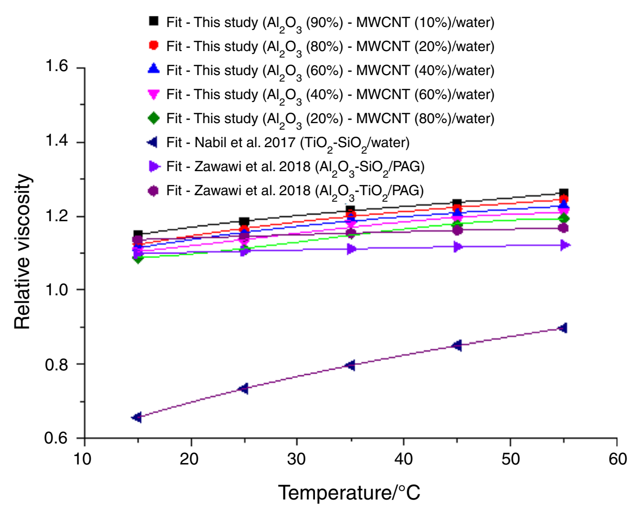

Fig. 14 Comparison of developed correlations (viscosity) to existing correlations at different temperatures

Correlation development

Studies have revealed the inability of classical/theoretical models to reasonably predict the thermophysical properties of nanofluids, which has led to the development of correlations to estimate nanofluids' thermal properties [43–45, 60]. The recent formulation of hybrid nanofluids with improved properties calls for the increased need to propose correlations for predicting their thermal properties. The experimental data (μ_{rel} and σ_{rel}) obtained in this study for the Al_2O_3–MWCNT/DIW nanofluids were fitted using regression analysis to formulate correlations to predict these properties as a function of temperature (Table 2).

Table 3 depicts the developed correlations, coefficients of regression, and determination for the μ_{rel} and σ_{rel} of the Al_2O_3–MWCNT/DIW nanofluids at various PMRs as a function of temperature. The ranges of the coefficients of regression and determination were 0.960–0.997 and 0.920–0.991, and 0.909–1.000 and 0.989–0.998, for the σ_{rel} and μ_{re}, respectively. Since literature is scarce on the μ_{eff} of hybrid nanofluids, the correlation derived (from experimental data) by Ganguly et al. [58] was used to compare the obtained experimental σ_{rel} data. Figure 13 shows the curve fittings of the obtained experimental data of σ_{rel} and that of Ganguly et al. [58] correlation. The fitted curves demonstrated slight enhancements of the σ_{rel} with increasing temperature and PMR of Al_2O_3 nanoparticles. The formula proposed by Ganguly et al. [58] was observed to closely estimate the σ_{rel} of Al_2O_3–MWCNT/DIW nanofluid with PMR of 20:80.

The curve fittings of the μ_{rel} data for this work and those of previous studies used for comparison purposes are presented in Fig. 14. The experiment-derived correlations from the works of Nabil et al. [68] and Zawawi et al. [69] were fitted and compared to the fitted data garnered for this study. From Fig. 14, it can be noticed that the curves fitted from the correlations proposed for SiO_2-TiO_2/water and Al_2O_3–SiO_2/PAG nanofluids could not fit the obtained μ_{rel} data, thus, it underestimated it. However, the Al_2O_3–TiO_2/PAG nanofluid correlation relatively estimated the experimental μ_{rel} data for the Al_2O_3–MWCNT/DIW nanofluid with PMR of 20:80 between 35 and 55 °C. Evidently, the proposed correlations for estimating the μ_{rel} and σ_{rel} of Al_2O_3–MWCNT/DIW nanofluid at different PMRs as given in Table 3 would be a good tool for the design of energy systems and processes.

Conclusions

A novel study on the measurement of σ_{eff} and μ_{eff} of stable Al_2O_3–MWCNT/DIW nanofluid ($\varphi = 0.1$ vol%) at different PMRs under varying temperatures was conducted. The addition of the hybrid nanoparticles at different PMRs to the DIW led to the enhancement of σ_{eff} and μ_{eff} of which a significant effect was observed on the σ_{eff}. Temperature rise significantly detracted μ_{eff}, but it slightly enhanced σ_{eff}. Both PMR and temperature had a contributory effect on the σ_{eff} and μ_{eff} of Al_2O_3–MWCNT/DIW nanofluids. The hybrid nanofluid with PMR of 90:10 was noticed to possess the highest augmentation of σ_{eff} (442.9%) and μ_{eff} (26.3%) at 55 °C, when compared with DIW. Increasing the PMR of MWCNT nanoparticles was observed to favor the reduction of μ_{eff} by 6.19% and 7.08% while its decrease aggravated σ_{eff} by 154.94% and 160.45% at 15 °C and 55 °C, respectively. The Al_2O_3–MWCNT/DIW nanofluids had a lower μ_{eff} in comparison with other hybrid nanofluids, especially at a lower PMR of MWCNT nanoparticles and temperature, which favored their application as coolants in heat exchangers.

Acknowledgements The funding received from the National Research Foundation of South Africa under the Renewable and Sustainable Energy Doctoral Scholarships is hereby acknowledged and appreciated.

References

1. Masuda H, Ebata A, Teramae K, Hishinuma N. Alteration of thermal conductivity and viscosity of liquid by dispersing ultra-fine particles. Netsu Bussei. 1993;7(4):227–33. https://doi.org/10.2963/jjtp.7.227.
2. Eastman JA, Choi SUS, Li S, Yu W, Thompson LJ. Anomalously increased effective thermal conductivities of ethylene glycol-based nanofluids containing copper nanoparticles. Appl Phys Lett. 2001;78:718–20. https://doi.org/10.1063/1.1341218.
3. Choi SUS, Eastman JA. Enhancing thermal conductivity of fluids with nanoparticles. ASME Int Mech Eng Congr Expo. 1995;66:99–105. https://doi.org/10.1115/1.1532008.
4. Lee S, Choi SUS, Li S, Eastman JA. Measuring thermal conductivity of fluids containing oxide nanoparticles. J Heat Transf. 1999;121:280–9. https://doi.org/10.1115/1.2825978.
5. Li Q, Xuan Y, Wang J. Experimental investigations on transport properties of magnetic fluids. Exp Therm Fluid Sci. 2005;30:109–16. https://doi.org/10.1016/j.expthermflusci.2005.03.021.
6. Prasher R, Song D, Wang J, Phelan P. Measurements of nanofluid viscosity and its implications for thermal applications. Appl Phys Lett. 2006;89:1–4. https://doi.org/10.1063/1.2356113.
7. Abareshi M, Sajjadi SH, Zebarjad SM, Goharshadi EK. Fabrication, characterization, and measurement of viscosity of α-Fe_2O_3-glycerol nanofluids. J Mol Liq. 2011;163:27–32. https://doi.org/10.1016/j.molliq.2011.07.007.
8. Namburu PK, Kulkarni DP, Misra D, Das DK. Viscosity of copper oxide nanoparticles dispersed in ethylene glycol and water mixture. Exp Therm Fluid Sci. 2007;32:397–402. https://doi.org/10.1016/j.expthermflusci.2007.05.001.
9. Adio SA, Sharifpur M, Meyer JP. Factors affecting the pH and electrical conductivity of MgO–ethylene glycol nanofluids. Bull Mater Sci. 2015;38:1345–57. https://doi.org/10.1007/s12034-015-1020-y.
10. Sharifpur M, Yousefi S, Meyer JP. A new model for density of nanofluids including nanolayer. Int Commun Heat Mass Transf. 2016;78:168–74. https://doi.org/10.1016/j.icheatmasstransfer.2016.09.010.
11. Shoghl NS, Jamali J, Moraveji KM. Electrical conductivity, viscosity, and density of different nanofluids: an experimental study. Exp Therm Fluid Sci. 2016;74:339–46. https://doi.org/10.1016/j.expthermflusci.2016.01.004.
12. NietoDeCastro CA, Murshed SMS, Lourenço MJV, Santos FJV, Lopes MLM, França JMP. Enhanced thermal conductivity and specific heat capacity of carbon nanotubes ionanofluids. Int J Therm Sci. 2012;62:34–9. https://doi.org/10.1016/j.ijthermalsci.2012.03.010.
13. Fal J, Barylyak A, Besaha K, Bobitski YV, Cholewa M, Zawlik I, Szmuc K, Cebulski J, Żyła G. Experimental investigation of electrical conductivity and permittivity of SC-TiO_2-EG nanofluids. Nanoscale Res Lett. 2016;11:1–9. https://doi.org/10.1186/s11671-016-1590-7.
14. Adio SA, Sharifpur M, Meyer JP. Influence of ultrasonication energy on the dispersion consistency of Al_2O_3–glycerol nanofluid based on viscosity data, and model development for the required ultrasonication energy density. J Exp Nanosci. 2016;11:630–49. https://doi.org/10.1080/17458080.2015.1107194.
15. Said Z. Thermophysical and optical properties of SWCNTS nanofluids. Int Commun Heat Mass Transf. 2016;78:207–13. https://doi.org/10.1016/j.icheatmasstransfer.2016.09.017.
16. Abdolbaqi MK, Mamat R, Sidik NAC, Azmi WH, Selvakumar P. Experimental investigation and development of new correlations for heat transfer enhancement and friction factor of bioglycol/water based TiO_2 nanofluids in flat tubes. Int J Heat Mass Transf. 2017;108:1026–35. https://doi.org/10.1016/j.ijheatmasstransfer.2016.12.024.
17. Abdolbaqi MK, Azmi WH, Mamat R, Sharma KV, Najafi G. Experimental investigation of thermal conductivity and electrical conductivity of bioglycol–water mixture based Al_2O_3 nanofluid. Appl Therm Eng. 2016;102:932–41. https://doi.org/10.1016/j.applthermaleng.2016.03.074.
18. Nor S, Azis N, Jasni J, Kadir M, Yunus R, Yaakub Z. Investigation on the electrical properties of palm oil and coconut oil based TiO_2 nanofluids. IEEE Trans Dielectr Electr Insul. 2017;24:3432–42. https://doi.org/10.1109/TDEI.2017.006295.
19. Jana S, Salehi-Khojin A, Zhong WH. Enhancement of fluid thermal conductivity by the addition of single and hybrid nano-additives. Thermochim Acta. 2007;462(1–2):45–55. https://doi.org/10.1016/j.tca.2007.06.009.
20. Suresh S, Venkitaraj KP, Selvakumar P, Chandrasekar M. Synthesis of Al_2O_3-Cu/water hybrid nanofluids using two step method and its thermo physical properties. Colloids Surf A Physicochem Eng Asp. 2011;388:41–8. https://doi.org/10.1016/j.colsurfa.2011.08.005.
21. Abbasi SM, Rashidi A, Nemati A, Arzani K. The effect of functionalisation method on the stability and the thermal conductivity

of nanofluid hybrids of carbon nanotubes/gamma alumina. Ceram Int. 2013;39:3885–91. https://doi.org/10.1016/j.ceramint.2012.10.232.
22. Tariq S, Ali H, Akram M. Thermal applications of hybrid phase change materials (HPCMs)—a critical review. Therm Sci. 2020;24:2151–69. https://doi.org/10.2298/tsci190302112t.
23. Tariq SL, Ali HM, Akram MA, Janjua MM, Ahmadlouydarab M. Nanoparticles enhanced phase change materials (NePCMs)—a recent review. Appl Therm Eng. 2020;2020:115305. https://doi.org/10.1016/j.applthermaleng.2020.115305.
24. Minea AA. Pumping power and heat transfer efficiency evaluation on Al_2O_3, TiO_2 and SiO_2 single and hybrid water-based nanofluids for energy application. J Therm Anal Calorim. 2020;139:1171–81. https://doi.org/10.1007/s10973-019-08510-3.
25. Esfe HM, Saedodin S, Biglari M, Rostamian H. Experimental investigation of thermal conductivity of CNTs-Al_2O_3/water: a statistical approach. Int Commun Heat Mass Transf. 2015;69:29–33. https://doi.org/10.1016/j.icheatmasstransfer.2015.10.005.
26. Esfe HM, Saedodin S, Yan WM, Afrand M, Sina N. Erratumto: study on thermal conductivity of water-based nanofluids with hybrid suspensions of CNTs/Al_2O_3 nanoparticles. J Therm Anal Calorim. 2016;124:455–60. https://doi.org/10.1007/s10973-016-5423-9.
27. Esfe HM, Sarlak MR. Experimental Investigation of switchable behavior of CuO-MWCNT (85%–15%)/10 W-40 hybrid nano-lubricants for applications in internal combustion engines. J Mol Liq. 2017;242:326–35. https://doi.org/10.1016/j.molliq.2017.06.075.
28. Kakavandi A, Akbari M. Experimental investigation of thermal conductivity of nanofluids containing of hybrid nanoparticles suspended in binary base fluids and propose a new correlation. Int J Heat Mass Transf. 2018;124:742–51. https://doi.org/10.1016/j.ijheatmasstransfer.2018.03.103.
29. Asadi A, Asadi M, Rezaniakolaei A, Rosendahl LA, Afrand M, Wongwises S. Heat transfer efficiency of Al_2O_3-MWCNT/thermal oil hybrid nanofluid as a cooling fluid in thermal and energy management applications: an experimental and theoretical investigation. Int J Heat Mass Transf. 2018;117:474–86. https://doi.org/10.1016/j.ijheatmasstransfer.2017.10.036.
30. Minea AA. A review on electrical conductivity of nanoparticle-enhanced fluids. Nanomaterials. 2019;9:1–22. https://doi.org/10.3390/nano9111592.
31. Rostami S, Nadooshan AA, Raisi A. An experimental study on the thermal conductivity of new antifreeze containing copper oxide and graphene oxide nano-additives. Powder Technol. 2019;345:658–67. https://doi.org/10.1016/j.powtec.2019.01.055.
32. Giwa SO, Sharifpur M, Meyer JP. Experimental study of thermo-convection performance of hybrid nanofluids of Al_2O_3-MWCNT/water in a differentially heated square cavity. Int J Heat Mass Transf. 2020;148:119072. https://doi.org/10.1016/j.ijheatmasstransfer.2019.119072.
33. Esfe MH, Arani AAA, Rezaie M, Yan WM, Karimipour A. Experimental determination of thermal conductivity and dynamic viscosity of Ag–MgO/water hybrid nanofluid. Int Commun Heat Mass Transf. 2015;66:189–95. https://doi.org/10.1016/j.icheatmasstransfer.2015.06.003.
34. Dardan E, Afrand M, Isfahani AHM. Effect of suspending hybrid nano-additives on rheological behavior of engine oil and pumping power. Appl Therm Eng. 2016;109:524–34. https://doi.org/10.1016/j.applthermaleng.2016.08.103.
35. Kannaiyan S, Boobalan C, Umasankaran A, Ravirajan A, Sathyan S, Thomas T. Comparison of experimental and calculated thermophysical properties of alumina/cupric oxide hybrid nanofluids. J Mol Liq. 2017;244:469–77. https://doi.org/10.1016/j.molliq.2017.09.035.
36. Akilu S, Baheta AT, Mior MA, Minea AA, Sharma KV. Properties of glycerol and ethylene glycol mixture based SiO_2-CuO/C hybrid nanofluid for enhanced solar energy transport. Sol Energy Mater Sol Cells. 2018;179:118–28. https://doi.org/10.1016/j.solmat.2017.10.027.
37. Rostami S, Nadooshan AA, Raisi A. The effect of hybrid nano-additive consists of graphene oxide and copper oxide on rheological behavior of a mixture of water and ethylene glycol. J Therm Anal Calorim. 2020;139:2353–64. https://doi.org/10.1007/s10973-019-08569-y.
38. Chereches EI, Minea AA. Electrical conductivity of new nanoparticle enhanced fluids: an experimental study. Nanomaterials. 2019;9:1–15. https://doi.org/10.3390/nano9091228.
39. Alarifi IM, Alkouh AB, Ali V, Nguyen HM, Asadi A. On the rheological properties of MWCNT-TiO_2/oil hybrid nanofluid: an experimental investigation on the effects of shear rate, temperature, and solid concentration of nanoparticles. Powder Technol. 2019;355:157–62. https://doi.org/10.1016/j.powtec.2019.07.039.
40. Gangadevi R, Vinayagam BK. Experimental determination of thermal conductivity and viscosity of different nanofluids and its effect on a hybrid solar collector. J Therm Anal Calorim. 2019;136:199–209. https://doi.org/10.1007/s10973-018-7840-4.
41. Goodarzi M, Toghraie D, Reiszadeh M, Afrand M. Experimental evaluation of dynamic viscosity of ZnO–MWCNTs/engine oil hybrid nanolubricant based on changes in temperature and concentration. J Therm Anal Calorim. 2019;136:513–25. https://doi.org/10.1007/s10973-018-7707-8.
42. Mechiri SK, Vasu V, Gopal AV. Investigation of thermal conductivity and rheological properties of vegetable oil based hybrid nanofluids containing Cu–Zn hybrid nanoparticles. Exp Heat Transf. 2017;30:205–17. https://doi.org/10.1080/08916152.2016.1233147.
43. Hamid KA, Azmi WH, Nabil MF, Mamat R, Sharma KV. Experimental investigation of thermal conductivity and dynamic viscosity on nanoparticle mixture ratios of TiO_2–SiO_2 nanofluids. Int J Heat Mass Transf. 2018;116:1143–52. https://doi.org/10.1016/j.ijheatmasstransfer.2017.09.087.
44. Aparna Z, Michael M, Pabi SK, Ghosh S. Thermal conductivity of aqueous Al_2O_3/Ag hybrid nano fluid at different temperatures and volume concentrations: an experimental investigation and development of new correlation function. Powder Technol. 2019;343:714–22. https://doi.org/10.1016/j.powtec.2018.11.096.
45. Wole-Osho I, Okonkwo EC, Adun H, Kavaz D, Abbasoglu S. An intelligent approach to predicting the effect of nanoparticle mixture ratio, concentration and temperature on thermal conductivity of hybrid nanofluids. J Therm Anal Calorim. 2020. https://doi.org/10.1007/s10973-020-09594-y.
46. Ghodsinezhad H, Sharifpur M, Meyer JP. Experimental investigation on cavity flow natural convection of Al_2O_3–water nanofluids. Int Commun Heat Mass Transf. 2016;76:316–24. https://doi.org/10.1016/j.icheatmasstransfer.2016.06.005.
47. Ho CJ, Liu WK, Chang YS, Lin CC. Natural convection heat transfer of alumina-water nanofluid in vertical square enclosures: an experimental study. Int J Therm Sci. 2010;49:1345–53. https://doi.org/10.1016/j.ijthermalsci.2010.02.013.
48. Garbadeen ID, Sharifpur M, Slabber JM, Meyer JP. Experimental study on natural convection of MWCNT-water nanofluids in a square enclosure. Int Commun Heat Mass Transf. 2017;88:1–8. https://doi.org/10.1016/j.icheatmasstransfer.2017.07.019.
49. Joshi P, Pattamatta A. An experimental study on buoyancy induced convective heat transfer in a square cavity using multi-walled carbon nanotube (MWCNT)/water nanofluid. In: Journal of physics: conference series, vol 745, no 1, p 032033. 2016. https://doi.org/10.1088/1742-6596/745/3/032033.
50. Suresh S, Venkitaraj KPP, Selvakumar P, Chandrasekar M. Effect of Al_2O_3–Cu/water hybrid nanofluid in heat transfer. Exp Therm

Fluid Sci. 2012;38:54–60. https://doi.org/10.1016/j.expthermflusci.2011.11.007.

51. Popiel CO, Wojtkowiak J. Simple formulas for thermophysical properties of liquid water for heat transfer calculations (from 0 to 150 °C). Heat Transf Eng. 1998;19:87–101. https://doi.org/10.1080/01457639808939929.
52. Solomon AB, van Rooyen J, Rencken M, Sharifpur M, Meyer JP. Experimental study on the influence of the aspect ratio of square cavity on natural convection heat transfer with Al_2O_3/water nanofluids. Int Commun Heat Mass Transf. 2017;88:254–61. https://doi.org/10.1016/j.icheatmasstransfer.2017.09.007.
53. Kumar PG, Kumaresan V, Velraj R. Stability, viscosity, thermal conductivity, and electrical conductivity enhancement of multiwalled carbon nanotube nanofluid using gum arabic. Fullerenes Nanotub Carbon Nanostruct. 2017;25:230–40. https://doi.org/10.1080/1536383X.2017.1283615.
54. Menbari A, Alemrajabi AA, Ghayeb Y. Investigation on the stability, viscosity and extinction coefficient of CuO–Al_2O_3/water binary mixture nanofluid. Exp Therm Fluid Sci. 2016;74:122–9. https://doi.org/10.1016/j.expthermflusci.2015.11.025.
55. Zawrah MF, Khattab RM, Girgis LG, El Daidamony H, Aziz REA. Stability and electrical conductivity of water-base Al_2O_3 nanofluids for different applications. HBRC J. 2016;12:227–34. https://doi.org/10.1016/j.hbrcj.2014.12.001.
56. Mehrali M, Sadeghinezhad E, Rashidi MM, Akhiani AR, Latibari ST, Mehrali M, Metselaar HSC. Experimental and numerical investigation of the effective electrical conductivity of nitrogen-doped graphene nanofluids. J Nanopart Res. 2015;17:1–17. https://doi.org/10.1007/s11051-015-3062-x.
57. Khdher AM, Sidik NAC, Hamzah WAW, Mamat R. An experimental determination of thermal conductivity and electrical conductivity of bio glycol based Al_2O_3 nanofluids and development of new correlation. Int Commun Heat Mass Transf. 2016;73:75–83. https://doi.org/10.1016/j.icheatmasstransfer.2016.02.006.
58. Ganguly S, Sikdar S, Basu S. Experimental investigation of the effective electrical conductivity of aluminum oxide nanofluids. Powder Technol. 2009;196:326–30. https://doi.org/10.1016/j.powtec.2009.08.010.
59. Sundar LS, Shusmitha K, Singh MK, Sousa ACM. Electrical conductivity enhancement of nanodiamond-nickel (ND-Ni) nanocomposite based magnetic nanofluids. Int Commun Heat Mass Transf. 2014;57:1–7. https://doi.org/10.1016/j.icheatmasstransfer.2014.07.003.
60. Giwa SO, Sharifpur M, Goodarzi M, Alsulami H, Meyer JP. Influence of base fluid, temperature, and concentration on the thermophysical properties of hybrid nanofluids of alumina—ferrofluid: experimental data, modeling through enhanced ann, anfis, and curve fitting. J Therm Anal Calorim. 2020;2020:0123456789. https://doi.org/10.1007/s10973-020-09372-w.
61. Qing SH, Rashmi W, Khalid M, Gupta TCSM, Nabipoor M, Hajibeigy MT. Thermal conductivity and electrical properties of hybrid SiO_2–graphene naphthenic mineral oil nanofluid as potential transformer oil. Mater Res Express. 2017;4:015504. https://doi.org/10.1088/2053-1591/aa550e.
62. Sharifpur M, Adio SA, Meyer JP. Experimental investigation and model development for effective viscosity of Al_2O_3-glycerol nanofluids by using dimensional analysis and GMDH-NN methods. Int Commun Heat Mass Transf. 2015;68:208–19. https://doi.org/10.1016/j.icheatmasstransfer.2015.09.002.
63. Esfe MH, Raki HR, Emami MRS, Afrand M. Viscosity and rheological properties of antifreeze based nanofluid containing hybrid nano-powders of MWCNTs and TiO_2 under different temperature conditions. Powder Technol. 2019;342:808–16. https://doi.org/10.1016/j.powtec.2018.10.032.
64. Giwa SO, Sharifpur M, Meyer JP. Effects of uniform magnetic induction on heat transfer performance of aqueous hybrid ferrofluid in a rectangular cavity. Appl Therm Eng. 2020;170:115004. https://doi.org/10.1016/j.applthermaleng.2020.115004.
65. Sundar LS, Singh MK, Sousa ACM. Turbulent heat transfer and friction factor of nanodiamond-nickel hybrid nanofluids flow in a tube: an experimental study. Int J Heat Mass Transf. 2018;117:223–34. https://doi.org/10.1016/j.ijheatmasstransfer.2017.09.109.
66. Sundar LS, Sousa ACM, Singh MK. Heat transfer enhancement of low volume concentration of carbon nanotube-Fe_3O_4/water hybrid nanofluids in a tube with twisted tape inserts under turbulent flow. J Therm Sci Eng Appl. 2015;7:021015. https://doi.org/10.1115/1.4029622.
67. Halelfadl S, Mare T, Estelle P. Efficiency of carbon nanotubes water based nanofluids as coolants. Exp Therm Fluid Sci. 2014;53:104–10. https://doi.org/10.1016/j.expthermflusci.2013.11.010.
68. Nabil MF, Azmi WH, Hamid KA, Mamat R, Hagos FY. An experimental study on the thermal conductivity and dynamic viscosity of TiO_2–SiO_2 nanofluids in water: ethylene glycol mixture. Int Commun Heat Mass Transf. 2017;86:181–9. https://doi.org/10.1016/j.icheatmasstransfer.2017.05.024.
69. Zawawi NNM, Azmi WH, Redhwan AAM, Sharif MZ, Samykano M. Experimental investigation on thermo-physical properties of metal oxide composite nanolubricants. Int J Refrig. 2018;89:11–21. https://doi.org/10.1016/j.ijrefrig.2018.01.015.